Eur. Phys. J. E (2015) **38**: 58
DOI 10.1140/epje/i2015-15058-7

THE EUROPEAN PHYSICAL JOURNAL E

Regular Article

Nanorheology of adsorbed polymer chains immersed in pure solvent

Fabrice Lapique[1], Jean Pierre Montfort[2], and Christophe Derail[2,a]

[1] SINTEF, Pb. 124 Blindern, NO-0314 Oslo, Norway
[2] Université de Pau et des Pays de l'Adour, IPREM UMR CNRS 5254, Equipe de Physique et Chimie des Polymères, 2, Avenue du Président Angot, F-64053 Pau, France

Received 24 January 2015 and Received in final form 24 April 2015
Published online: 23 June 2015 –

Abstract. Long linear chains of polybutadiene are adsorbed on the two surfaces of a surface force apparatus and immersed in pure tetradecane. The hydrodynamic force was measured by drainage experiments and by frequency sweeps at constant distances. We related the hydrodynamic thickness to the chain dimension. The complex modulus encompasses the shear modulus and, at distances lower than the hydrodynamic thickness, a compression modulus. The compression term was related to the static force which appears when the two adsorbed layers are overlapped. The complex shear modulus was interpreted by a two-components hydrodynamic model proposed by P. Sens *et al.* We first complemented the theoretical model. Then, our experimental data fit the proposed viscoelastic expressions in the entire range of distances. The storage modulus is supposed to be affected by a residue of free chains and by the dispersion of the loop lengths.

1 Introduction

The interest of measuring the forces acting between solid surfaces coated with polymers originates from the comprehension of colloidal stability and rheology. Numerous static and dynamic force measurements have been conducted with surface force apparatuses [1–11]. Some of them deal with a spectroscopy in a large range of frequencies able to explore simultaneously various components of the hydrodynamic forces. The main findings are: a static repulsive force at short distances, a drainage force variation which determines a hydrodynamic thickness of the polymer layers —both characteristic distances are of the order of 4 to 10 times the radius of gyration of the free chains— and a compression term in the complex elastic modulus arising at the same distances. The hydrodynamic component of the complex modulus shows an increase of viscosity and average relaxation time with the degree of confinement.

Some authors attempt to interpret experimental data in the framework of a continuous description of the viscoelastic polymer layers. For melts, Montfort [12] extends the expression of the lubrication force exerted by a homogeneous viscous fluid to a viscoelastic heterogeneous one. No relation was made locally between the viscoelastic behaviour and the conformation of the adsorbed chains. Experimental data were found to be consistent with a description in terms of multiple uniform layers [10]. For end-grafted chains immersed in a good solvent, Fredrickson and Pincus [13] assimilate the network created by the polymer layer with a porous medium. Therefore, the drag of the solvent through that network is approximated by a Brinkman equation [14]. The mesh size of the porous medium is replaced by a local correlation length which depends on the monomer concentration profile. The authors establish the expression of the hydrodynamic force when the monomer concentration is constant within the polymer layer. A more realistic parabolic profile [15,16] could be used but we do not know about more recent work on that field.

For irreversibly adsorbed polymer layers, Sens, Marques and Joanny [17] adopt the same view as Fredrickson and Pincus. The main difference comes from the expression of the correlation length. They use the scaling picture introduced by de Gennes [18] where an adsorbed layer is described as a self-similar grid. Therefore, the correlation length varies linearly with the distance z from the surface. The monomer concentration profile does not impact directly the permeability term of the Brinkman equation.

This paper deals with an experimental study of adsorbed polybutadiene (PB) layers immersed in tetradecane which is a good solvent of PB. First, the paper from Sens *et al.* is complemented. Then, we present the surface force apparatus and the samples. The experimental data and the theoretical predictions are compared and discussed.

[a] e-mail: christophe.derail@univ-pau.fr

2 Theoretical aspects

We summarize the main contribution of a theoretical study of the viscoelasticity of adsorbed polymer layers conducted by P. Sens *et al.* [17]. In that paper, some results are presented by graphics without the related analytical expressions. Some others expressions are only valid at large separations h_0. Therefore, we are presenting a complete version of the expressions of the complex shear modulus of adsorbed and confined polymer layers.

The viscoelastic properties of the confined solution are described within the framework of a two-components hydrodynamic model. The two components are the solvent and the polymer loops. Hydrodynamically, the solvent is viewed as a Newtonian fluid and the elastic network of the loops experiences a friction force coming from the relative motion of the solvent. The drag of the solvent through the network creates a viscous dissipation and an elastic strain on the polymer. The drag is described by the Brinkman equation which approximates the adsorbed polymer layers by a porous medium with a local permeability $\mu(z)$ proportional to $\eta/\xi^2(z)$. As the local correlation length $\xi(z)$ scales as the distance z to the wall, Sens *et al.* define a dimensionless number l such as $\mu(z) = l(l-1)\eta/z^2$. The number l measures the friction between the solvent and the polymer and is larger than unity. The friction vanishes when $l = 1$. Therefore, the hydrodynamic equation for the solvent flow inside the layers is

$$\eta\nabla^2\mathbf{v}_l - \mu(z)\left(\mathbf{v}_l - \dot{\mathbf{u}}\right) - \nabla P = 0, \tag{1}$$

where $\mathbf{v}$ is the solvent velocity field and $\mathbf{u}$ is the polymer displacement field.

The behaviour of the pure solvent between the layers is given by a Stokes equation

$$\eta\nabla^2\mathbf{v}_s - \nabla P = 0. \tag{2}$$

The equation of motion of the polymer expresses the balance between the elastic stress of the network and the friction with the solvent:

$$\nabla(E(z)\nabla\mathbf{u}) + \mu(z)\left(\mathbf{v} - \dot{\mathbf{u}}\right) = 0, \tag{3}$$

where $E(z)$ is the local Young modulus. In a scaling approach, the elastic modulus is proportional to the osmotic pressure, that is to say $E(z) \cong \alpha k_B T/z^3$ with α being a numerical factor.

Within the Derjaguin approximation, the above equations reduce to

$$\eta\partial_z^2 v_{pr} - \eta\frac{l(l-1)}{z^2}\left(v_{pr} - \dot{u}_r\right) - \partial_r P = 0, \tag{4}$$

$$\eta\partial_z^2 v_{sr} - \partial_r P = 0, \tag{5}$$

$$\partial_z\left(\frac{\alpha k_B T}{z^3}\partial_z u_r\right) + \eta\frac{l(l-1)}{z^2}\left(v_{pr} - \dot{u}_r\right) = 0. \tag{6}$$

Therefore, the solvent velocity and the polymer displacement fields are deduced from the above coupled equations as a function of the pressure gradient.

The solvent incompressibility equation can be written as $\nabla\mathbf{v} = 0$ *or* $\partial_z v_z - (1/r)\partial_r(rv_r) = 0$. The integration over r leads to the relation $2v_r = -r\partial_z v_z$. A second integration over the gap gives

$$2\int_0^h v_r\,\mathrm{d}z = -rV(t). \tag{7}$$

The resolution of the four above equations lead to an expression of the pressure gradient as a function of the upper surface velocity $V(t)$. The hydrodynamic normal force is obtained by integration of the stress tensor over the surface:

$$\begin{aligned} F &= \int_0^\infty 2\pi r\left[P(r) - P_\infty - \eta(\partial_z v_z)_{z=0}\right]\mathrm{d}r \\ &= 2\pi R\int_{h_0}^\infty \left[P(h) - \eta(\partial_z v_z)_{z=0}\right]\mathrm{d}h. \end{aligned} \tag{8}$$

As it is assumed that no sliding motion occurs on the surfaces, the expression of the hydrodynamic force is

$$F = 2\pi R\int_{h_0}^\infty P(h)\mathrm{d}h. \tag{9}$$

We are going to concentrate the analysis on harmonic displacements of the upper surface which allows us to deal with complex quantities. If we state that the imposed displacement of the upper surface is $U^*(t) = U\exp(i\omega t)$, the complex amplitude of the hydrodynamic force $F^*(\omega)$ is related to the complex shear modulus by [4]:

$$F^*(\omega) = 6\pi R^2\frac{U}{h_0}G^*(\omega). \tag{10}$$

Therefore, the complex shear modulus will be expressed by

$$G^*(\omega) = \frac{h_0}{3RU}\int_{h_0}^\infty P^*(h)\mathrm{d}h. \tag{11}$$

Sens *et al.* suggest to calculate the velocity field by a perturbation method relatively to ω; the lowest order allows the calculation of the loss modulus G'' and the first correction that of the storage modulus G'.

The related complex equations are

$$\eta\partial_z^2 v^*{}_{pr} - \eta\frac{l(l-1)}{z^2}\left(v^*{}_{pr} - i\omega u\right) - \partial_r P^* = 0, \tag{12}$$

$$\eta\partial_z^2 v^*{}_{sr} - \partial_r P^* = 0, \tag{13}$$

$$\partial_z\left(\frac{\alpha k_B T}{z^3}\partial_z u\right) + \eta\frac{l(l-1)}{z^2}v''{}_{pr} = 0, \tag{14}$$

$$4\int_0^{h/2} v^*{}_r\,\mathrm{d}z = -i\omega rU. \tag{15}$$

Equations (12), (14), (15) give the complex velocity and pressure gradient fields. The polymer displacement field is deduced from eq. (14). The complex shear modulus will be deduced from the pressure field by eq. (11).

The solutions of the above equations need to know various boundary conditions. Two situations have to be considered:

1) The two layers are separated by the pure solvent when the separation of the two surfaces h_0 is higher than twice the thickness of each layer R_F ($h_0 > 2R_F$). Assuming a no-slip condition of the polymer on the solid surfaces, the polymer network is not deformed ($u(z=0)=0$) and there is no elastic stress at the edge of the layers ($\partial_z u(z = R_F) = 0$). At the edge of the layers, the velocity and the stress are continuous (${v^*}_{pr} = {v^*}_{sr}$; $\partial_z {v^*}_{pr} = \partial_z {v^*}_{sr}$ for $z = R_F$). For symmetry reasons, $\partial {v^*}_{sr} = 0$ at the midplane ($z = h/2$).

2) The two layers are overlapped ($h_0 < 2R_F$) in the central region of the gap. The boundary conditions are identical in the outer region ($h > 2R_F$). In the central part ($h_0 < h < 2R_F$), the conditions at $z = R_F$ have to be replaced by the same conditions at $z = h/2$.

The velocity fields are given in Sens paper (with a minor error in eq. (29) therein). In appendix A, we give the expressions of the various pressure gradient fields. We deduce the complex shear modulus for overlapped and non-overlapped layers from eq. (11).

2.1 Non-overlapping layers

The loss modulus is expressed by

$$G''_{no} = 2\eta\omega x_0 \int_{x_0}^{\infty} (x - x_0) f(x) \mathrm{d}x \tag{16}$$

with $x = h/R_F$ and $x_0 = h_0/R_F$.

The storage modulus is given by

$$G'_{no} = \frac{3\eta^2\omega^2 x_0 R_F^3}{\alpha k_B T} \frac{(l-1)^2}{(l+1)(l+3)} \int_{x_0}^{\infty} (x - x_0) f(x) g(x) \mathrm{d}x \tag{17}$$

with $f(x)$ and $g(x)$ given in appendix A.

Sens *et al.* [17] express the storage and loss modulus respectively in the asymptotic form ($x_0 \gg 1$) in agreement with the above expressions:

$$G'(\omega) \approx \frac{(l-1)^2}{4\alpha k_B T (l+1)(l+3)} \omega^2 \eta^2 \frac{R_F^4}{h_0},$$

$$G''(\omega) \approx \omega\eta \left(1 + \frac{2(l-1)}{l} \frac{R_F}{h_0}\right).$$

The second term of the loss modulus $G''_2 = \omega\eta \frac{2(l-1)}{l} \frac{R_F}{h_0}$ stands for the polymer contribution. Therefore Sens defines a relaxation time τ such as

$$\tau = \frac{G'}{\omega G''_2} \propto \frac{\eta R_F^3}{k_B T}, \tag{18}$$

which scales as the relaxation time of the large loops with a size of the order of R_F. This simple argument emphasizes the fact that, at low frequency, the contribution of the polymer to the viscoelasticity of the fluid is dominated by the large loops.

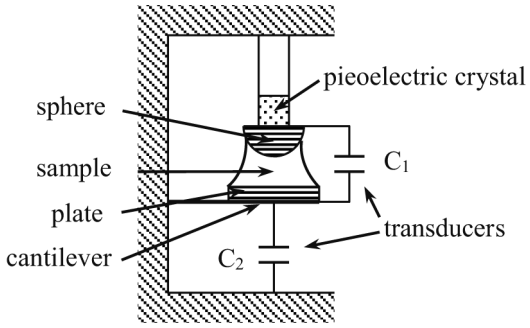

Fig. 1. Diagram of the SFA equipment.

2.2 Overlapping layers

The two polymer layers are overlapped at distances h_0 lower than $h_l = 2R_F$ or $x_0 \leq 2$.

Within the outer region ($h > 2R_F$), the velocity, pressure gradient and polymer displacement fields are the same as in a non-overlapping gap. The velocity profile within the inner region ($h < 2R_F$) is obtained by replacing the boundary condition at $z = R_F$ by a symmetry condition at the midplane. The expressions of the pressure gradient are given in appendix A.

The loss modulus is written as:

$$G''_{ov} = \omega\eta \left[2x_0 \int_2^{\infty} (x - x_0) f(x) \mathrm{d}x + \frac{l(l+1)^2}{4(l+3)} (x_0 - 2)^2\right]. \tag{19}$$

The storage modulus is

$$G'_{ov} = \frac{3\omega^2\eta^2 x_0 R_F^3}{\alpha k_B T} \frac{(l-1)^2}{(l+1)(l+3)} \times \left[\int_2^{\infty} (x - x_0) f(x) g(x) \mathrm{d}x + k(l)(x_0 - 2)^2\right], \tag{20}$$

with $k(l)$ defined in appendix A.

In each expression, the first term accounts for the contribution of the outer part of the gap ($x_0 \geq 2$) and the second term accounts for the contribution of the inner part ($x_0 \leq 2$). Both expressions respect the continuity with the non-overlapping expressions at $x_0 = 2$.

3 Experimental

3.1 Technique

We have used a surface force apparatus as a dynamic rheometer by applying an oscillating strain to the sample, which is confined between a plate and a sphere. The sphere of radius R is vibrating in the vertical direction from a ground position at distance h_0 from the horizontal plate.

As sketched in fig. 1, the geometry of surface force machines is a space between plane and sphere with a separation h_0 much lower than the radius R of the sphere

(Derjaguin's approximation). Therefore, the local separation h at distance r from the axis satisfies:

$$h \approx h_0 + r^2/2R. \tag{21}$$

An axial motion imposed to the sphere with a velocity $V(t)$-and displacement $U(t)$-induces a normal force $F(R, h_0, V)$ on the plane, via the confined fluid. The plane is supposed fixed and no slippage occurs between the fluid and the non-deformable surfaces. As the flow will primarily occur in the radial direction, some approximations can be made on the velocity field inside the fluid: $v_r \gg v_z$, $v_r(r, z, t)$ and $v_z(z, t)$ and it is justified to consider $\partial_z \gg \partial_r$. The pressure gradient is essentially radial, $\nabla P \approx \partial_r P$.

Both substrates are made of fused silica (Young's modulus $E = 73\,\text{GPa}$, Poisson ratio $\nu = 0.17$) covered by a 60 nm thick layer of cobalt (Young's modulus $E = 209\,\text{GPa}$, Poisson ratio $\nu = 0.3$). The radius R of the sphere is of the order of 1 mm. The roughness is below 1 nm RMS and considered as negligible in our measurements.

The distance h_0 between the sphere and the plate will vary from about 30 nm to 200 nm. The amplitude U of the sphere oscillation is of the order of 1 to 2 nm so as to assure a linear response of the sample throughout the distance and frequency sweep. The experiments have been conducted at room temperature. The plate-sphere separation depends strongly on temperature. Therefore, the SFA has been confined in a home-made box which exhibits a temperature stability of about 0.01 °C at room temperature.

The raw mechanical impedance is a combination of the transfer function of the apparatus (response of the transducers and of the cantilever), of the stiffness of the stand, of the elastic deformation of the surfaces and of the viscoelastic behavior of the sample. A calibration of the two first components as been conducted systematically previous to each experiment. A study of the impact of the elastic deformation of the surfaces has been recently conducted by Leroy and Charlaix [19]. They define a critical distance D_k, below which a major perturbation appears. It is given by

$$D_k = 8R\left[\frac{(1-\nu^2)\eta\omega}{E}\right]^{\frac{2}{3}}. \tag{22}$$

In our experiments, the order of magnitude of D_k is given by $D_k \sim 0.01\omega^{2/3}$ by considering the substrates made of pure silica and a solvent viscosity of 3.3 mPa s. The highest value of frequency is $4000\,\text{s}^{-1}$ which gives for D_k a largest value of 2.5 nm. All our experiments are conducted at distances much larger than D_k, especially at low frequencies. Far above D_k, Leroy and Charlaix predict an elastic component of the hydrodynamic response of the force due to the deformation of the substrates. The expression of the related storage modulus is

$$G' = \frac{9\pi^2}{512}\eta\omega\left(\frac{D_k}{h_0}\right)^{3/2}, \tag{23}$$

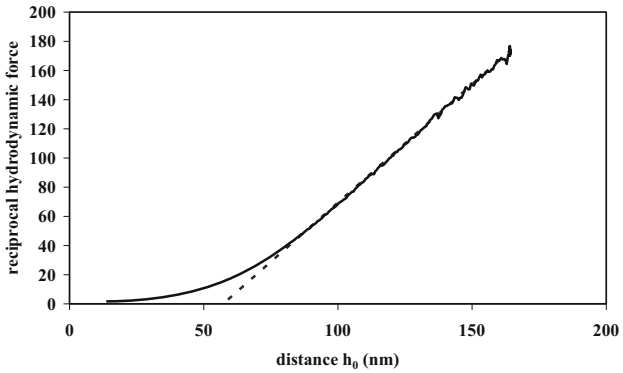

Fig. 2. Hydrodynamic force (N) *versus* distance plate/sphere (nm) obtained from a drainage experiments.

which gives

$$\frac{G'}{\omega^2} \approx 2 \cdot 10^{-7} h_0^{-3/2}, \tag{24}$$

with h_0 expressed in nm. We will see later than the distance dependence and the order of magnitude of G'/ω^2 in our experiments do not fit the above expression.

3.2 Samples

The polymer is a narrow polybutadiene from Polymer Laboratories ($M_w = 120\,000\,\text{g mol}^{-1}$, polydispersity index lower than 1.1, radius of gyration $R_g = 6.9\,\text{nm}$). It was diluted in tetradecane with a concentration far below the critical concentration. With the type of SFA we used [20], the two surfaces cannot be immerged in the solution. A droplet of solution was introduced in the gap and incubated during one day. The concentration was adjusted in order to allow the polymer chains to adsorb on both surfaces as a monolayer separated by pure solvent. The various parameters which have to be controlled are: the polymer concentration, which was obtained after several dilutions, the volume of the droplet and the gap height which determine the area covered by the polymer. We adopted that strategy because it is not possible to use a concentrate solution and to extract *in situ* the free solution to be replaced by pure solvent. Not either, pre-coated surfaces can be introduced in the machine as the determination of the contact position needs bare surfaces.

A way of checking whether the middle of the gap is free of polymer at large distances ($h_0 \sim R_g$) is to compare the viscosity for the pure solvent and for the solvent in presence of polymer layers. That was be done by drainage experiments (fig. 2). The hydrodynamic force was measured at a frequency of 38 Hz and at distances ranging from 13 nm to 170 nm. Several cycles were performed and showed a good reproducibility. Therefore, the adsorbance of the polymer chains is stable. The slope of the linear part (above 90 nm) gives a viscosity of 3.3 mPa s, which is twice the value of the pure tetradecane viscosity (1.7 mPa s). That means that a small amount of free chains are diluted in the solvent. We estimate the ratio of concentration c/c^*

($c^* \approx {R_g}^3$ is the limit concentration for dilute solutions) from a Rouse behaviour of the dilute solution of polymer. The viscosity law is

$$\eta - \eta_s = c\frac{N\zeta R_g^2}{6\pi^2}\sum_1^\infty \frac{1}{p^2}\,,$$

which leads to

$$\frac{c}{c^*} \approx 10^3 \frac{R_g(\eta - \eta_s)}{N\zeta}\,.$$

The monomeric friction coefficient ζ has been estimated of the order of $10^{-6}\,\mathrm{g\,s^{-1}}$ [21]. Therefore, the ratio c/c^* is of the order of 10^{-2} which means that the concentration of free chains is very low.

As tetradecane is a good solvent of polybutadiene, we assume the free chains not interact strongly with the loops and tails of the adsorbed chains. Furthermore, the extrapolation of the straight line at zero force defines a hydrodynamic thickness of the layers. The value of 29 nm is about four times the radius of gyration of melted chains. The gap may come from the good solvent which swells the chains and also from the presence of a small amount of free chains connected with the large loops of the adsorbed chains.

3.3 Experiments

At various distances ranging from 36 to 192 nm, a frequency sweep is performed in a range of 0.06 to $4000\,\mathrm{s^{-1}}$. The distance scan begins at the largest distances. A delay of some ten minutes is applied in order to reach an equilibrium. At the end of the frequency sweep, we checked the reproducibility for one frequency. The complex shear modulus $G^*(\omega)$ is deduced from the hydrodynamic force according to eq. (11). Two typical diagrams are presented hereafter (fig. 3).

At distances larger than the hydrodynamic thickness, the complex shear modulus is typical of a viscoelastic behaviour in the terminal zone of relaxation ($G' \propto \omega^2$ and $G'' \propto \omega$). The value of the viscosity $\eta = G''/\omega$ is higher than the solvent viscosity. The value of G'/ω^2 is higher of $3 \cdot 10^{-7}$ which is three orders of magnitude higher than the value expected for the signature of an elastic deformation of the substrates (eq. (24)). The accuracy of the storage modulus is poor, due to the low level of the elastic response.

At distances lower than the hydrodynamic thickness, the hydrodynamic complex shear modulus shows a better determination of the elastic component. At low frequencies, the storage modulus levels off. That additional modulus G_c, much higher than the hydrodynamic part in the low frequency range, comes from the compression of the overlapped polymer layers. As the distance is decreasing, G_c increases and will overcome the storage shear modulus in the whole range of frequencies.

The compression modulus G_c can be related to the static force (fig. 4) which appears when the two layers are overlapped. Sens *et al.* [17] express the static force from

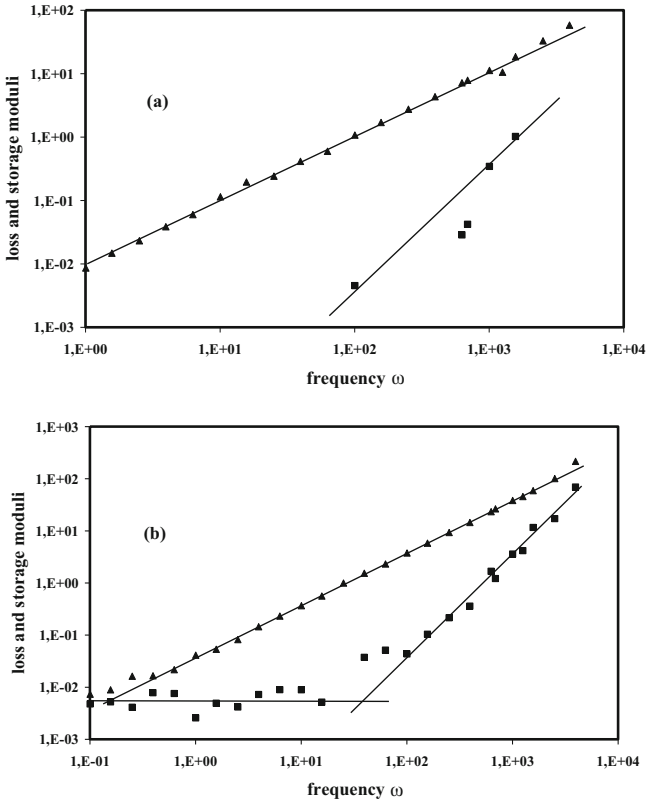

Fig. 3. Complex shear modulus (Pa) at two distances plate/sphere: 91.1 nm (a) and 46.1 nm (b). The sphere oscillates at fixed distance (G': square, G'': triangle).

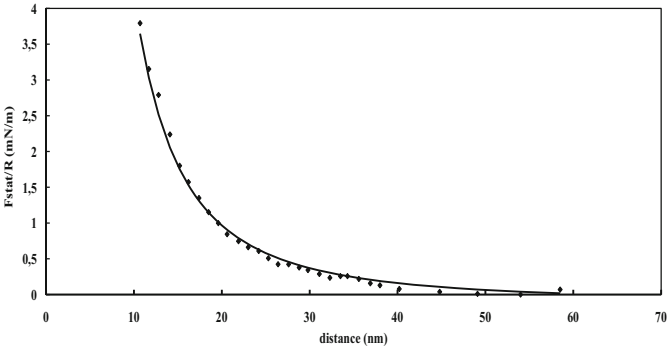

Fig. 4. Experimental static force (mN $\mathrm{m^{-1}}$) *versus* distance and fit with eq. (25).

the osmotic pressure of the polymer solution at the middle of the gap:

$$F_s \propto 2\pi R \int_{h_0}^{2R_F} \pi_{osm}(h/2)\mathrm{d}h$$
$$= K 8\pi R k_B T \left(\frac{1}{h_0^2} - \frac{1}{4R_F^2}\right). \qquad (25)$$

Our data fit the above expression at $T = 296\,\mathrm{K}$ with $R_F = 31.5\,\mathrm{nm}$ and a prefactor $K \approx 4$.

The value of the layer thickness is very close to the hydrodynamic one. It allows us to calculate the order of

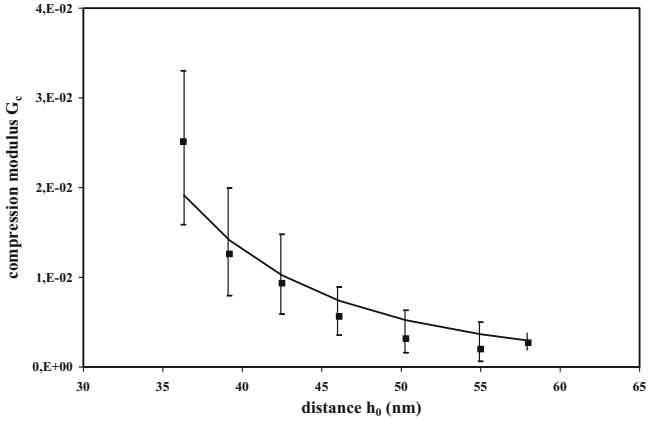

Fig. 5. Experimental compression modulus G_c (Pa) derived from experimental static force for overlapped layers and fit with eq. (26).

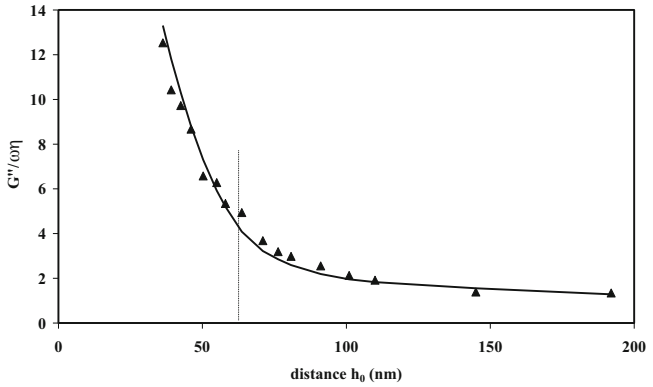

Fig. 6. Fit of the adimensional loss modulus with a value of $l = 6.7$ (eqs. (16), (19)).

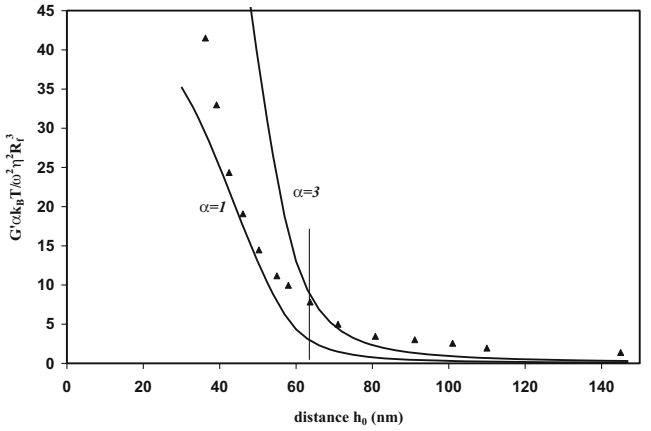

Fig. 7. Fit of the adimensional storage modulus with a value of $l = 6.7$ (eqs. (17), (20)).

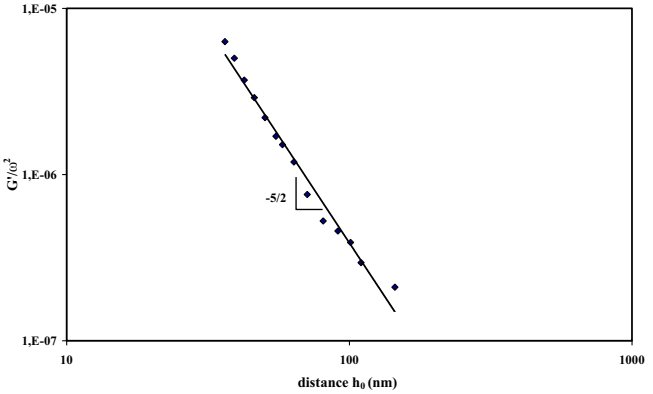

Fig. 8. Scaling law of G'/ω^2 with the distance plate/sphere.

magnitude of the loop relaxation time (eq. (18)) which is 10^{-5} s. Then the frequency range is such as $\omega\tau < 1$.

The variation of the compression modulus is deduced from the variation of the static force [6] by

$$G_c = \frac{h_0}{6\pi R^2}\frac{\mathrm{d}F_s}{\mathrm{d}h_0}\,. \tag{26}$$

The fit is correct as seen in fig. 5.

We are going to explore a weakly overlapping configuration where the storage modulus comes from the deformation of the polymer network due to the solvent flow. The range of distances encompasses both the overlapped and non-overlapped situations.

The adimensional loss modulus $G''/\omega\eta$ is well described by equations (16) and (19) for a factor $l = 6.7\pm0.8$ (fig. 6). The factor l is a measure of the degree of friction between the polymer and the solvent. We know only that there is no friction when $l = 1$.

The adimensional storage modulus $G'\alpha k_B T/\omega^2\eta^2 R_F^3$ depends on the prefactor α which accounts for the ratio between the osmotic pressure and the local polymer elasticity. According to the experimental data, that factor should range between 1 and 3 (fig. 7). At large distances, the data are rather scattered, therefore the determination of G'/ω^2 is not accurate.

We come back to the possible artefact in the values of the storage modulus due to the deformation of the substrate. Equation (24) expresses the contribution of the deformation of the substrate. It predicts its value and a $-3/2$ power law dependence with the distance. Figure 8 shows that the experimental exponent $(-5/2)$ is different from the predicted one. Moreover, the experimental values are higher by more than three orders of magnitude. We can conclude that, in our experiments, the deformation of the substrate does not affect the hydrodynamic modulus of the sample.

As a conclusion, the model proposed by Sens *et al.* seems to be relevant for describing the rheology of irreversibly adsorbed polymer layers separated by pure solvent. The agreement is good for the viscous part and less accurate for the elasticity. One reason may come from a scattering of the size of the large loops. It is well known that the steady-state compliance $J_e^0 = \frac{G'}{G''^2}$ at low frequency varies dramatically with the molecular-weight distribution in polydisperse polymer melts [22]. The viscosity of narrow and broad linear polymer melts with a same average weight is comparable but it is not true for the storage modulus. For adsorbed chains, the distribution of

loop and tail length is comparable with a dispersion of chain length in a linear melt. Some recent experiments on the hysteresis of compression of adsorbed polymer layers also show that the repulsive force is sensitive to the details of the structure [9]. Furthermore, the variation of the degree of overlapping of the large loops with distance modify the contribution of the non-overlapping loops, therefore it modifies the overall dispersity. The presence of a small amount of free chains can also contribute to overall elasticity.

4 Conclusion

We have conducted steady and oscillatory squeezing experiments of irreversibly adsorbed polybutadiene layers immersed in good solvent. The picture of their viscoelastic behavior proposed by Sens *et al.* seems to be validated by our experiments. The chains are considered as an elastic porous medium through which the solvent flows. The friction between the solvent and the polymer induces an extra viscous dissipation and an elastic deformation of the network formed by the polymer chains. When the two layers overlap each other, an extra finite elastic modulus appears. When that plateau modulus is subtracted from the elastic response, the complex shear modulus exhibits at low frequency a Maxwell-like behavior. The models works well for describing the loss modulus. It is less precise for the storage modulus. One reason could be a dispersity of the loop and tail sizes which induces a dispersion of the local layer thickness. That hypothesis can be tested by using end-grafted monodisperse chains which lead to a steper profile of the loops density. Another interesting point is the behavior at high frequency. Sens *et al.* propose to use a blob model. The blob size depends on the frequency and it is defined from the Zimm relaxation time. At distances lower than the blob size, the self-similar profile is valid. At distances higher than the blob size, the layer is equivalent to a solution of blobs. The authors use scaling arguments to predict frequency scaling laws of the storage and loss moduli. For our samples, the high frequency zone starts at $\omega \sim 10^5\,\mathrm{s}^{-1}$. As the highest frequency is of the order of 10^3 to $10^4\,\mathrm{s}^{-1}$, exploring the high frequency zone means to be able to build polymer layers ticker than 100 to 200 nm or to use solvents of higher viscosity.

Appendix A.

Equations (12) to (15) give the velocity, polymer displacement and pressure gradient fields.

The expressions of the velocity field for non-overlapping layers are given by Sens *et al.* as a function of the gradient pressure field:

v'_{pr} relation (15) of [17]
v'_{sr} relation (16) of [17]
v''_{pr} relation (30) of [17]
v''_{sr} relation (29) of [17]

(the factor $l-2$ in the denominator has to be replaced by $l+3$). We add the expression of the polymer displacement and the pressure gradient fields:

$$u = \frac{\partial_r P''}{\alpha k T}\frac{l(l-1)}{(l+1)(l-2)}\left[\frac{1}{5}z^5 + \frac{1}{(l-1)(l+3)} \times \left((1-l)R_F^{2-l} - \frac{(l+1)(2-l)}{2l}hR_F^{1-l}\right)z^{l+3} - \frac{(l+1)(2-l)}{8l(l-1)}hz^4\right], \tag{A.1}$$

$$\partial_r P'' = 6\eta\omega r U \frac{1}{h^3 - 6\frac{l-1}{l}R_F h^2 + 12\frac{l-1}{l+1}R_F^2 h - 8\frac{l(l-1)}{(l+1)^2}R_F^3} = 6\eta\omega r U\, f(h), \tag{A.2}$$

$$\partial_r P' = \frac{9\eta^2\omega^2 r U}{\alpha k T}\frac{(l-1)^2 R_F^4}{(l+1)(l+3)} f(h) g(h), \tag{A.3}$$

with

$$g(h) = \frac{h^2 - \frac{8l(2l+7)}{5(l+1)(l+4)}R_F h + \frac{8l^2(l+3)}{3(l+1)^2(l+4)}R_F^2}{h^3 - 6\frac{l-1}{l}R_F h^2 + 6\frac{2l^2-2l-1}{l(l+1)}R_F^2 h - 8\frac{l(l-1)}{(l+1)^2}R_F^3}. \tag{A.4}$$

Inside the overlapped layers, the velocity field is deduced from the above expressions by replacing R_F by $h/2$.

The expression of the complex pressure gradient is

$$\partial_r P'' = 6\eta\omega r U \frac{l(l+1)^2}{h^3(l+3)}, \tag{A.5}$$

$$\partial_r P' = \frac{6\eta^2\omega^2 r U}{\alpha k T}\frac{l^2(l-1)^2(l+1)(l^3+12l^2+51l+60)}{160(l+3)^2(l+4)} = \frac{6\eta^2\omega^2 r U}{\alpha k T}k(l). \tag{A.6}$$

Author contribution statement

Authors contributed equally to the paper.

References

1. J.J. Klein, J. Chem. Soc., Faraday Trans. **1, 79**, 99 (1983).
2. D.Y.C. Chan, R.G. Horn, J. Chem. Phys. **83**, 5311 (1985).
3. J.N. Israelachvili, Colloid Polym. Sci. **264**, 1060 (1986).
4. J.P. Montfort, G. Hadziioannou, J. Chem. Phys. **88**, 7187 (1988).
5. H.W. Hu, S. Granick, Science **258**, 1339 (1992).
6. E. Pelletier, J.P. Montfort, F. Lapique, J. Rheol. **38**, 1151 (1994).
7. E. Pelletier, J.P. Montfort, J.L. Loubet, A. Tonck, J.M. Georges, Macromolecules **28**, 1990 (1995).
8. G. Luengo, F.J. Schmitt, R. Hill, J. Israelachvili, Macromolecules **30**, 2482 (1997).
9. U. Raviv, J. Klein, T.A. Witten, Eur. Phys. J. E **9**, 405 (2002).
10. T. Drobek, N.D. Spencer, M. Heuberger, Macromolecules **12**, 5254 (2005).

11. C. Derail, F. Lapique, J.P. Montfort, Macromolecules **44**, 7438 (2011).
12. J.P. Montfort, Macromolecules **41**, 5024 (2008).
13. G.H. Fredrickson, P. Pincus, Langmuir **7**, 786 (1991).
14. H.C. Brickman, Appl. Sci. Res. **A1**, 27 (1947).
15. S.T. Milner, T.A. Witten, M.E. Cates, Macromolecules **21**, 2610 (1988).
16. C. Marzolin, P. Auroy, M. Deruelle, J.P. Folkers, L. Léger, A. Menelle, Macromolecules **34**, 8694 (2001).
17. P. Sens, C.M. Marques, J.F. Joanny, Macromolecules **27**, 3812 (1994).
18. P.G. de Gennes, Macromolecules **14**, 1637 (1981).
19. S. Leroy, E. Charlaix, J. Fluid Mech. **674**, 389 (2011).
20. J.P. Montfort, A. Tonck, J.L. Loubet, J.M. Georges, J. Polym. Sci. Part B **29**, 677 (1991).
21. W. Liu, Y. Yang, T. Hu, Polymer **29**, 1789 (1988).
22. J.P. Montfort, G. Marin, P. Monge, Macromolecules **19**, 1979 (1986).